

Classification, Distribution, and Fatigue Life of Pitting Corrosion for Aircraft Materials

R. M. Pidaparti,* S. Jayanti,[†] C. A. Sowers,[‡] and M. J. Palakal[§]
Purdue University at Indianapolis, Indianapolis, Indiana 46202

An investigation of the pitting corrosion classification, distribution, and prediction of corrosion-fatigue life of aircraft panels is carried out. A probabilistic neural network was developed to classify the pit size ranges and determine the distribution based on the available experimental data. The results obtained indicate that the pit sizes can be classified into three groups. The gamma distribution function fit the experimental data of pit size ranges quite well. A neural network model was also developed for predicting the fatigue life of aircraft panels subjected to corrosion-fatigue loading. The developed neural network model was validated against the experimental data and other analytical methods available in the literature. Overall, the predictions from this study demonstrate the usefulness of neural network approach over other analytical methods for determining the fatigue life of aircraft structures.

I. Introduction

FAILURES may result when aircraft components are operated in a corrosive environment due to nucleation, initiation, and propagation of cracks at the corrosion pits in aircraft materials. Wallace and Hoepfner¹ described many types of corrosion that may occur in aircraft structures. Lap joints are a common structural element in many military aircraft (KC-135, C-130, J-STARS) and in transport aircraft fuselages. These joints are subject to corrosion damage. Corrosion in lap joints results in material loss, pillow stresses, pillow cracks, rivet failures, and interactions with fatigue. Corrosion generally attacks the faying surfaces in lap joints and occurs when the adhesive bond/sealant between the layers breaks down, allowing moisture to penetrate. Pitting corrosion usually follows the general attack of corrosion on faying surfaces and may sometimes evolve into exfoliation corrosion.

It is well known that corrosion pitting has a strong effect on fatigue life of aluminum alloys used in aircraft structures.^{2–4} Fatigue cracks usually initiate from the corrosion pit sites. Under the interaction of cyclic load and the corrosive environment, cyclic loading facilitates the pitting process, and corrosion pits, acting as geometrical discontinuities, leading to crack initiation and propagation and then final failure. Usually, the fatigue crack initiation period includes crack (or pit) nucleation and early (or short) crack (or pit) growth. Nucleation of localized corrosion pitting modifies the local stress and may ultimately initiate cracks.

Pits almost always initiate at some chemical or physical heterogeneity at the surface, such as inclusions, second phase particles, flaws, mechanical damage, or dislocations. The aluminum alloys contain numerous constituent particles, which play an important role in corrosion pit formation.¹ To better understand particle-induced

pitting corrosion in 2024/T3 and 7075/T6 aluminum alloys, optical microscopy, scanning electron microscopy (SEM), and transmission electron microscopy (TEM) techniques have been used.² Because of an aircraft's special service environments, for example, salt water, electrochemical reactions are possible and corrosion pits are readily formed between the constituent particles and the surrounding matrix in these alloys.

Prediction of corrosion and corrosion fatigue is very important for the structural integrity of aircraft materials and structures. The presence of corrosion pits can significantly shorten the fatigue crack initiation life and decrease the threshold stress intensity of an alloy by as much as 50% (Ref. 3). To quantify pitting-induced corrosion fatigue, a critical pit size model⁴ has been proposed in which a corrosion fatigue crack is considered to have nucleated from a pit. The pit grows to a critical size when the local mechanical condition is adequate for the onset of crack growth. In a series of papers, Wei et al.⁵ and Harlow and Wei^{6–8} have developed a probabilistic model for the prediction of corrosion and corrosion fatigue life. Their model is based on the growth of a single dominant flaw from a pit, to a small surface crack, and then into a through crack. They showed that probabilistic concepts could be employed to predict the pitting corrosion fatigue process. However, in their model, fatigue crack nucleation was not considered. Rokhlin et al.⁹ developed a fracture mechanics model for fatigue crack initiation and propagation from single artificial and actual pits based on two different stress intensity factors. However, in their model, pit nucleation and growth were not considered.

Zamber and Hillberry¹⁰ recently developed an effective probabilistic approach for predicting fatigue life (based entirely on crack propagation) of corroded 2024/T3 aluminum, and the predictions were verified with experimental data. In their model, the crack initial life was assumed to be small compared with the total life and was neglected. This approach might lead to significant errors if both the applied cyclic stress and pitting corrosion level are low (i.e., there is a prolonged period of fatigue crack initiation life due to high-cycle fatigue¹¹), which may take a large portion of the total life. Recently, Wang et al.¹² presented a simple analytical and probabilistic model for predicting the corrosion fatigue life in aluminum alloys by considering all stages of the corrosion-fatigue process. The results obtained indicate that crack initiation life varies approximately 10–40% as compared to crack propagation life. Although much is understood regarding the growth stage of corrosion fatigue, there is little information regarding the initiation and growth stages of pitting corrosion from simulation models.

For the past few years, the investigators have been studying the structural integrity and durability issues related to aging aircraft structures and materials. To further understand and predict durability

Received 25 May 2001; revision received 22 September 2001; accepted for publication 10 December 2001. Copyright © 2002 by the American Institute of Aeronautics and Astronautics, Inc. All rights reserved. Copies of this paper may be made for personal or internal use, on condition that the copier pay the \$10.00 per-copy fee to the Copyright Clearance Center, Inc., 222 Rosewood Drive, Danvers, MA 01923; include the code 0021-8669/02 \$10.00 in correspondence with the CCC.

*Professor, Department of Mechanical Engineering, Purdue School of Engineering and Technology. Associate Fellow AIAA.

[†]Graduate Student, Department of Mechanical Engineering, Purdue School of Engineering and Technology; currently Ph.D. Student, Purdue University, West Lafayette, IN 47907. Member AIAA.

[‡]Undergraduate Student, Department of Mechanical Engineering, Purdue School of Engineering and Technology. Member AIAA.

[§]Professor and Chair, Department of Computer and Information Science, Purdue School of Science.

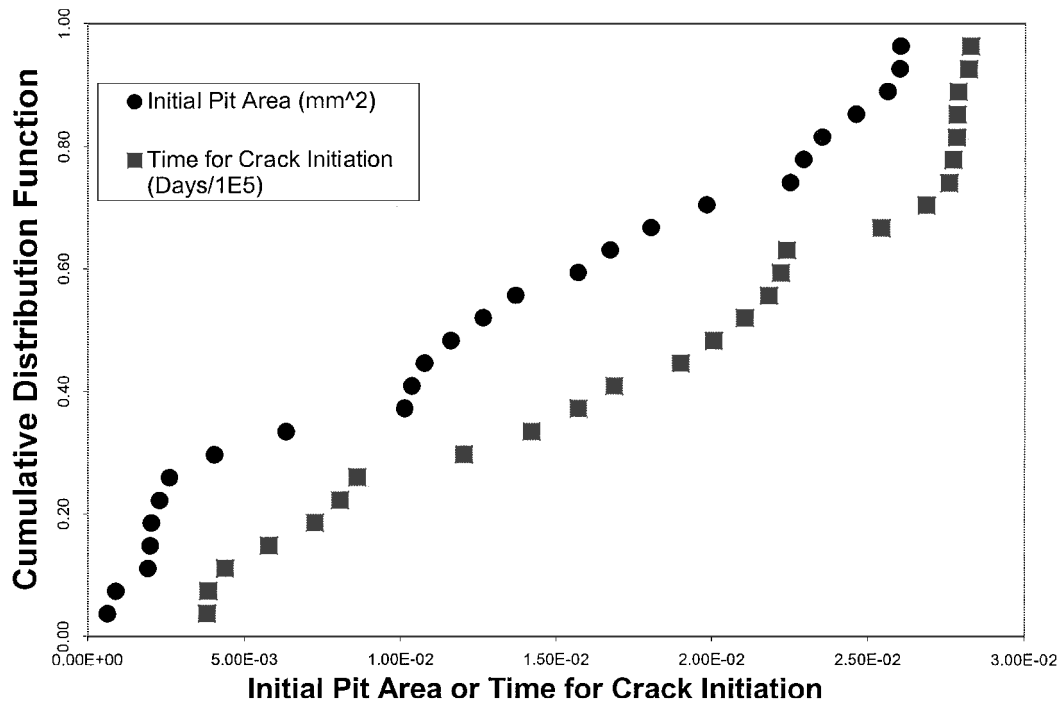


Fig. 1 Cumulative distribution function fits for initial pit area and the time for crack initiation for the pit area data reported by Zamber and Hillberry.¹⁰

issues of aging aircraft materials and structures, the problem of pitting corrosion and corrosion fatigue is investigated. Specifically, the present study is aimed at investigating the pitting corrosion classification, distribution, and prediction of corrosion-fatigue life using artificial neural network models. The results obtained are validated with existing experimental data and other analytical models.

II. Pit Size Classification

Because of the large distribution of pit sizes in aircraft materials, it may be necessary to use several distribution functions rather than a single distribution function to represent initial pit characteristics found in the literature. For example, the experimental data of Zamber and Hillberry¹⁰ indicated that pit sizes ranged in area from 629 to 26,017 μm^2 . In many probabilistic models of aircraft aluminum corrosion, a single probability distribution is often used to represent initial corrosion pit characteristics. Based on available data, this practice appears inaccurate because one function cannot properly represent an entire range of pit data. For example, Fig. 1 shows the cumulative distribution function for the pit area data ($n = 26$) reported by Zamber and Hillberry.¹⁰ The calculated times for crack initiation (for pit growth) based on the work of Harlow and Wei⁸ are also shown in Fig. 1 for comparison. It can be seen from Fig. 1 that it is very difficult to fit a single distribution function to the data of either pit area or the time for crack initiation. Accurate distribution fits can be achieved if the pit size data range is classified into smaller groups. Therefore, one of the objectives of this study is to classify the pits according to size and find a best probabilistic fit for the classified pit distributions.

With regard to the classification of pit growth, it can be seen from the data presented in Fig. 1 that there is an obvious need to classify the pit growth into various groups/regions, so that a valid distribution function can be fitted to the experimental data. The classification of pit growth is carried out using probabilistic neural networks. A brief introduction to probabilistic neural networks is presented hereafter for clarity.

Probabilistic neural networks (PNN) are software-based models inspired by the decision-making and problem-solving processes of biological nervous systems. The PNN have been used for the purposes of classification, mapping, and associative memory.¹³ PNN have been used successfully to classify electrocardiograms as either normal or abnormal, to identify ship hulls from sonar data,

to determine sheep eating phases based on sound recordings, to identify gemstones based on spectral information, and to classify many other data sets based on image or sound data (URL: http://www.maths.uwa.edu.au/~rkealley/ann_all/ann_all.html).

In this study, MATLAB's[®] PNN function was used to classify initial pit sizes. In MATLAB,¹³ the training data set is entered as a single row matrix, and the corresponding target data set is entered as a separate single row matrix. These two matrices are then fed to the NEWPNN function for training. On training, the network is ready to receive new data for classification. In the present study, a PNN was used to classify the corrosion pits based on pit sizes, as well as length of time for crack initiation. Note, however, that the pits are assumed to be circular in cross section. The pit size used in this study is defined as the radius of a circular pit with the same area as that of the pit seen on a real specimen.

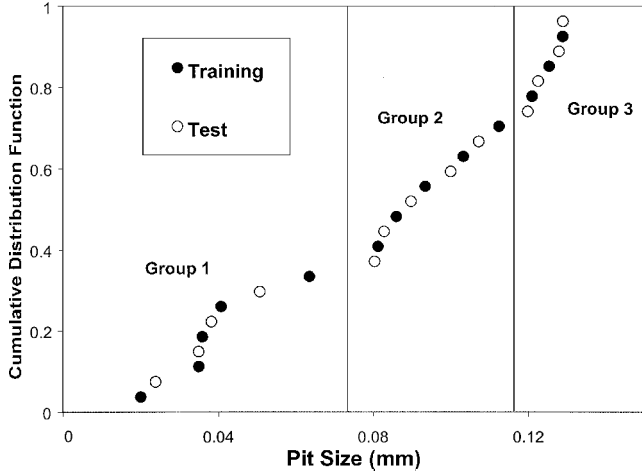
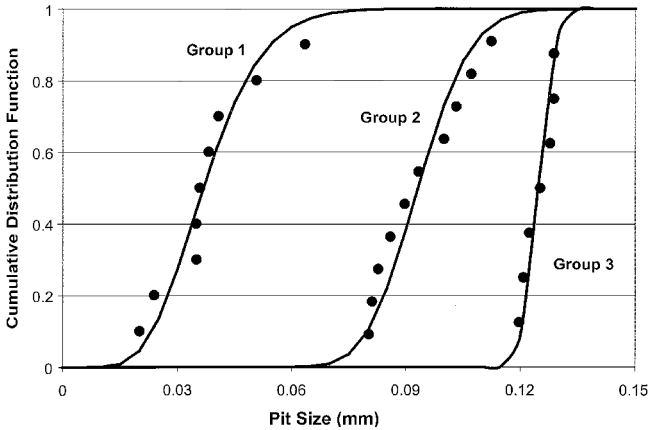
A PNN is developed to classify the pit size data reported by Zamber and Hillberry¹⁰ into three groups. Based on the results presented in Fig. 1, it appears that the data fit naturally into three groups. These groups are numbered 1–3, with group 1 representing the shortest length of time for crack initiation (380–860 days), and group 3 representing the longest (2541–2826 days). Half of the data points were used to train the network, with either pit size (defined by radius by assuming the pit to be of circular shape) or time for crack initiation as the input and classification group number as the output from the network. The network training and testing results of pit size classification are shown in Fig. 2. Note from Fig. 2 that the developed probabilistic network is able to classify the pit size data reasonably well. However, more data are needed for further classification and testing using the developed network. To extend the results of this study, additional pit size and/or time for crack initiation data could be incorporated to create continuous data ranges.

III. Pit-Growth Probability Distributions

Based on a review of the literature, we selected the gamma, normal, and Weibull probability distributions to determine which function provides the best representation of the data and determine their fit to each of the pit size classification groups. MATLAB's probability toolbox was utilized to fit functions, and time data were normalized by dividing by 10^4 before performing the fits. The gamma, normal, and Weibull distributions used in this study are defined according to Eqs. (1), (2), and (3), respectively. These distributions can be found in the statistical toolbox in MATLAB software.

Table 1 Cumulative distribution parameters for the three classified pit size ranges

Group	Gamma			Normal			Weibull		
	a	b	r^2	μ	σ	r^2	a	b	r^2
1	9.63	$3.95E-03$	0.936	$3.80E-02$	$1.31E-02$	0.928	$3.35E+04$	3.30	0.928
2	74.8	$1.25E-03$	0.964	$9.36E-02$	$1.15E-02$	0.963	$1.76E+09$	9.19	0.952
3	1260	$1.00E-04$	0.934	0.125	$3.79E-03$	0.937	$3.43E+08$	9.53	0.953

**Fig. 2** Probabilistic neural network results of training and testing for initial pit size classification, based on the data reported by Zamber and Hillberry.¹⁰**Fig. 3** Gamma distribution function fits for the three classified initial pit size ranges.

Gamma distribution function,

$$p = F(x | a, b) = \frac{1}{b^a \Gamma(a)} \int_0^x t^{a-1} \exp\left(-\frac{t}{b}\right) dt \quad (1)$$

Normal distribution function,

$$p = F(x | \mu, \sigma) = \frac{1}{\sigma \sqrt{2\pi}} \int_{-\infty}^x \exp\left[-\frac{(t-\mu)^2}{2\sigma^2}\right] dt \quad (2)$$

Weibull distribution function,

$$p = F(x | a, b) = \int_0^x abt^{b-1} \exp(-at^b) dt \quad (3)$$

The results of distribution functions and their constants are summarized in Table 1. The results of best fit (gamma distribution function) for the three classification groups are shown in Fig. 3. Overall, the gamma distribution function fits well with the three classified groups based on the r^2 values. It is evident from Fig. 3 that it may be

necessary to use several distribution functions rather than a single distribution function to represent initial pit characteristics due to the large distribution of pit sizes in aircraft materials.

IV. Corrosion-Fatigue Neural Network Model

Corrosion fatigue is a process and is an outcome of synergistic interactions among the environment, material microstructure, and cyclic loads. The goal of this study is to explore the possibility of using neural network models for predicting the fatigue life of aging aircraft panels affected by corrosion-fatigue damage. It is anticipated that the development of neural network models will complement the existing analytical, experimental, and numerical methods. Neural networks are computational models that can obtain knowledge of a process by training with sample input and known output data. Backpropagation neural networks are very popular for approximating nonlinear relationships. Different types of networks have been used successfully to model the behavior of engineering problems.

Just as the most important part of any physical modeling process is the proper selection of the parameters involved, the same is also true of the neural network methodology. Because the neural network models predict the output parameter as a function of the input parameters, it is of utmost importance to choose all of the proper causal parameters that have a significant effect on the output parameter and characterize the phenomena uniquely. At the same, it must be kept in mind that, although neural networks have been thought of as black boxes, selecting too many (insignificant) parameters may adversely affect the training of the neural network. Hence, for proper application of this approach, the input parameters have to be chosen carefully to achieve a reasonable model of the process.

The most important factors that determine the corrosion-fatigue life of the panels are the fatigue loading and corrosion environment. Fatigue loading is characterized by maximum stress amplitude $\Delta\sigma$, stress ratio R , and the frequency of loading f . The duration of exposure D_{exp} of the material to the corrosive environment is also considered in developing the neural network model. Apart from the external parameters, the geometry of the crack is also a very important factor for accurately modeling the corrosion fatigue mechanism. The critical pit size a_{ci} , defined as the pit size when a crack initiates and begins to grow from a corrosion pit that can be measured by SEM and TEM techniques in the laboratory, is used in the present model and is shown in Fig. 4. The initial pit size a_0 represents the material heterogeneity and manufacturing quality of the structural component. The final crack size a_f , before failure (as defined by the user or the inspection criteria), is also used as one of the input parameters. The final crack size is associated with the failure condition, the experimental termination condition, or the replacement or repair condition of the panel. However, in this study, it represents the detectable crack size, which can be measured by nondestructive techniques like eddy current or ultrasound that will help in the maintenance planning of the aging aircraft components. It is necessary to define the initiation life at this point, which is defined as the number of load cycles it takes for an initial pit of size a_0 to grow to a critical size a_{ci} , after which it transforms into a crack. Similarly, the propagation life is the number of loading cycles required for the initiated crack of size a_{ci} to grow to a final failure size of a_f .

A multilayer, feedforward neural network with a backpropagation learning algorithm was used in this study. Figure 5 shows the schematic representation of the neural network model developed and the parameters affecting the corrosion-fatigue behavior. A total of seven parameters were used to model both the corrosion and

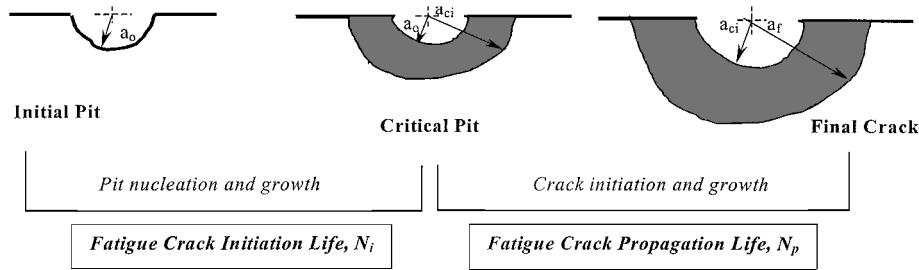


Fig. 4 Schematic of the corrosion fatigue crack growth defining critical pit size.

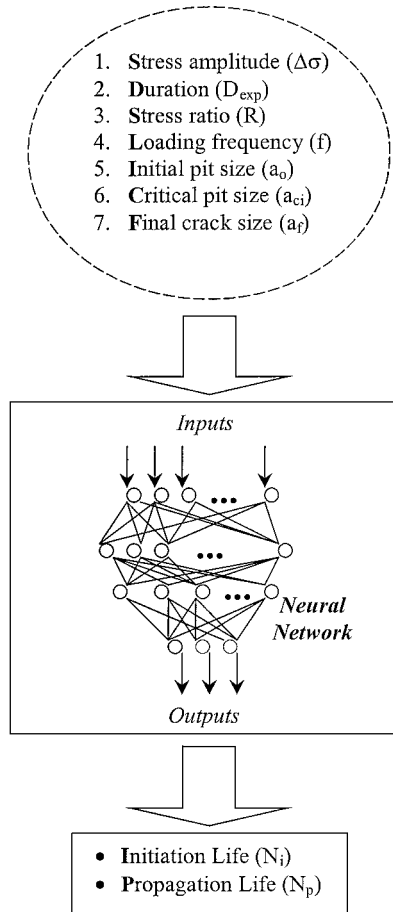


Fig. 5 Schematic of neural network architecture and the input/output parameters affecting the corrosion-fatigue behavior of aircraft panels.

fatigue phenomena and were chosen as input to the neural network model. Both the initiation life (defined as the number of load cycles it takes for a pit to grow to a size required for crack initiation) and the propagation life (defined as the number of load cycles required to grow an initial crack to failure) were used as the outputs for the neural network model to see how they are affected by the various input parameters.

The data for the network was obtained from various studies published in the literature.^{6,9,10} Because there was a lack of sufficient data quantifying the initiation and propagation lives separately, the analytical equations suggested by Wang et al.¹² were used to complement the missing life data (either initiation or propagation life) for training. The reason behind using these equations is that these equations take into account the nucleation of pit, whereas other analytical methods do not consider the pit nucleation in the initiation life. Hence, the neural network was trained with a total failure life identical to the experimental values, but with an initial life as predicted by equations.¹² Each of the input variables was normalized so that all of the data lie between 0 and 1, which is recommended for proper training of neural networks. A set of nine specimens was

set aside for validating the developed neural network. The results obtained for these specimens are presented in the following sections.

A. Sensitivity Study

A relatively large scatter, of several orders of magnitude (10^2 – 10^5), was observed in the pit sizes and experimental lives of the panels presented as the training set. This limits the ability of the neural network to train reasonably. Hence, the initiation life, propagation life, as well as the critical pit size values, were normalized after taking their logarithm with base 10. The training improved considerably after this numerical adjustment.

Once the proper input and output parameters have been selected for modeling the corrosion-fatigue process, the network architecture (number of hidden layers and nodes) has to be determined to achieve a model that simulates the process accurately. The process of obtaining the best network is often a trial and error process. Hence, the final network has to be determined after a number of trials. The search for the best network is done by initially choosing a small network architecture and subsequently increasing the number of nodes until the mean square error for training is reasonably low and the outputs correlate well with the experimental data for the validation set. The final network, chosen after several trials with various architectures by changing the number of hidden layer neurons, consisted of nine nodes in the first hidden layer and four nodes in the second hidden layer.

B. Training and Validation

The neural network was trained with the data available for corrosion fatigue in the literature. The network converged to a target mean square error of 0.001 after 9660 epochs. The correlation of the predicted life after training vs the life predicted by the analytical equations, as well as experimental data, is presented in Fig. 6. The comparisons of the neural network predicted initiation and propagation life is shown in Figs. 6a and 6b, respectively.

The network was validated for a total of nine test specimens. Two test specimens were those obtained from the results of Harlow and Wei.⁸ The predictions of the neural network are compared with those of Harlow and Wei⁸ in Table 2. The term N_f in Table 2 is defined as $N_i + N_p$. It can be observed from Table 2 that the predictions of the present model are closer to the results of Harlow and Wei for the final failure lives. Predictions of N_i (initiation life), N_p (propagation life), and N_f (total fatigue life, $N_i + N_p$) for two more test specimens from Rokhlin et al.⁹ are compared in Table 3, which indicates that the present model is closer to the experimental results as compared to Wang et al.¹² for both of the test cases. The prediction is also better than the predictions of Rokhlin et al.⁹ for one test case with a critical pit size a_{ci} of 375 μm .

The predictions of the remaining five test specimens are compared with the experimental data and analytical equations in Table 4. The details of predictions (i.e., the sources of the data, the loading, and the environmental conditions) are also given in Table 4. It can be observed from Table 4 that the neural network predictions are closer to the experimental failure life for most of the test specimens, whereas the initiation life for all of the specimens is also close to those of Wang et al.¹² The results presented in Tables 2–4 and the comparisons between various sources of data indicate the generality and utility of the neural network developed for predicting the corrosion fatigue life of aging aircraft panels.

Table 2 Comparison of neural network prediction for fatigue initiation and failure life for test specimens made of Al 2024-T3 alloy⁸ subjected to fatigue loading with $\Delta\sigma = 90$ MPa, $f = 10$ Hz, and $R = -1$

Pit/crack length, mm	Harlow and Wei ⁸		Neural network prediction	
	N_i, N_f	N_i/N_f	N_i, N_f	N_i/N_f
$a_{ci} = 0.074$	10,100 (N_i)	0.15	20,169 (N_i)	0.23
$a_f = 1.0$	68,100 (N_f)	0.15	86,708 (N_f)	0.23
$a_{ci} = 0.106$	30,100 (N_i)	0.39	46,746 (N_i)	0.48
$a_f = 1.0$	77,600 (N_f)	0.39	98,246 (N_f)	0.48

Table 3 Comparison of neural network predictions for total fatigue failure life N_f of test specimens made of Al 2024-T3 alloy⁹ subjected to fatigue loading with $\Delta\sigma = 206$ MPa, $f = 15$ Hz, and $R = 0.2$

Critical pit depth a_{ci} , μm	Experimental data (Rokhlin et al. ⁹)	Analytical prediction (Rokhlin et al. ⁹)	Analytical prediction (Wang et al. ¹²)	Neural network prediction
170	$3.40E+05$	$3.50E+05$	$6.61E+04$	$4.27E+05$
375	$2.20E+05$	$2.40E+05$	$1.90E+04$	$2.25E+05$

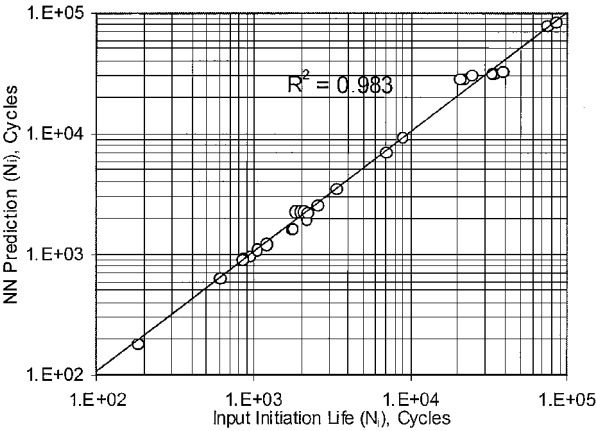


Fig. 6a Comparison of initiation life for training set between neural network prediction and the network input for initiation life.

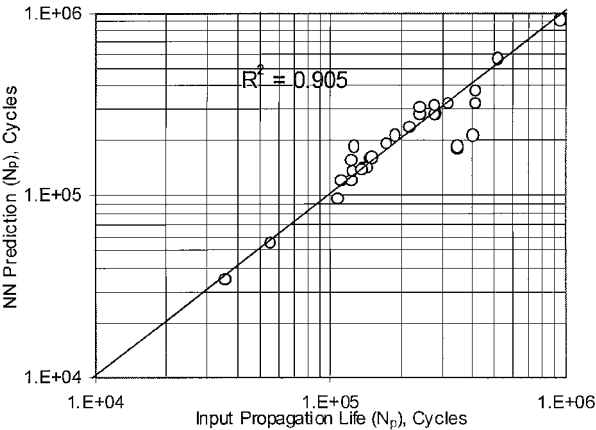


Fig. 6b Comparison of propagation life for training set between neural network prediction and the network input for propagation life.

C. Simulation Results

To observe the effects of the various input parameters on the fatigue life of the panels, several cases were simulated using the trained neural network. In this study, the effects of three parameters (pit size, stress amplitude, and frequency of loading) on the fatigue life were obtained. The neural network predicted results are compared to the other available results in the literature. The simulation results are briefly described hereafter.

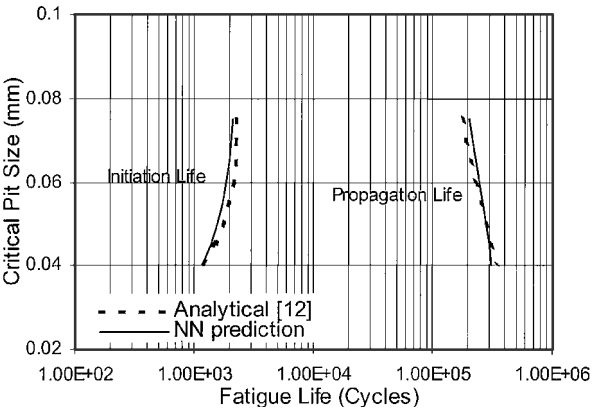


Fig. 7a Comparison of initiation and propagation life between neural network predictions and the analytical model of Wang et al.¹²

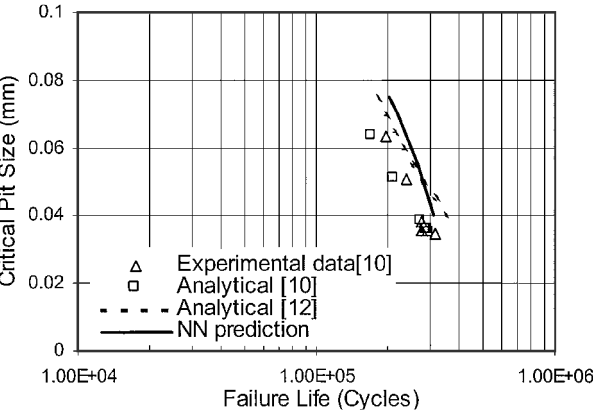


Fig. 7b Comparison of fatigue life between neural network predictions and the analytical models and experimental data.

1. Pit Size

The effect of increasing the critical pit size (from 0.04 to 0.075 mm) and the corresponding fatigue life predicted for an Al 2024-T3 aluminum panel was studied. Other parameters for this simulation are $\Delta\sigma = 198$ MPa, $f = 10$, $R = 0.1$, $a_f = 3$ mm, and $a_0 = 0.001$ mm. The duration of exposure D_{exp} was 144 h. The simulation results are presented in Fig. 7. Note from Fig. 7a that there is an increase of initiation life from 1171 to 2125 cycles as the pit size is increased from 0.04 to 0.075 mm. However, the propagation life is predicted to decrease from 3.1×10^5 to 2.02×10^5 cycles for the same increase in the pit size. Figure 7b shows the result of total fatigue life from the neural network simulation and is compared with the available experimental data and analytical methods. A reasonably good agreement is seen between the neural network prediction and the experimental data.

2. Stress Amplitude

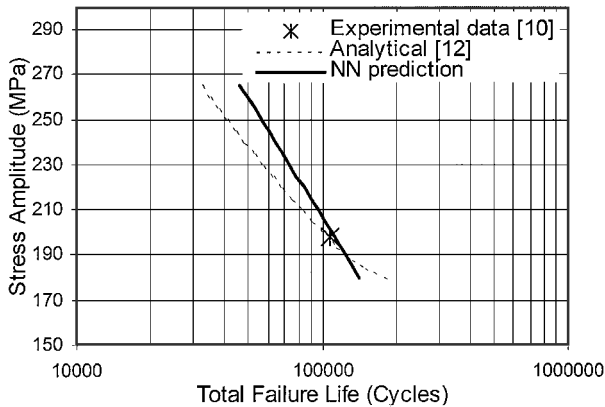
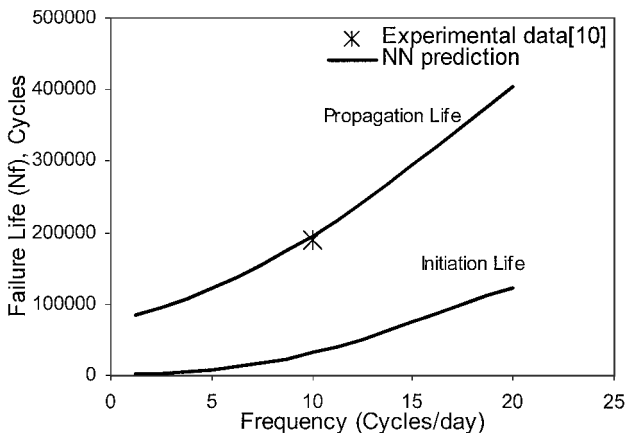
The effect of increasing the stress amplitude (from 180 to 265 MPa) and the corresponding fatigue life predicted for an Al 2024-T3 aluminum panel was examined. Other parameters for this simulation are the same as those just given. The neural network predicted fatigue life is shown in Fig. 8, along with existing experimental data and analytical solutions. However, the total failure life predicted by the neural network is more conservative as compared to the analytical method for a lower stress amplitude and less conservative for a higher stress amplitude, as can be seen from Fig. 8. The failure life of the panel decreased from 1.41×10^5 to 4.62×10^4 cycles when the stress amplitude was increased from 180 to 265 MPa.

3. Frequency of Fatigue Loading

To predict the effect of varying frequency of fatigue loading on the fatigue life, a simulation was carried out where the frequency of

Table 4 Comparison of neural network model predictions of fatigue life for test data

Source/Ref.	Stress amplitude $\Delta\sigma$, MPa	Duration of exposure D_{exp} , h	Frequency f , cycles/day	Final crack length a_f , mm	Critical pit size a_{ci} , mm	Experimental data		Neural network prediction		
						N_i	N_f	N_i	N_p	N_f
10	198	144	10	3	0.024	—	3.06×10^5	3.37×10^2	3.06×10^5	3.06×10^5
10	198	144	10	3	0.086	—	1.52×10^5	2.21×10^3	1.73×10^5	1.75×10^5
10	180	192	10	3	0.125	—	1.98×10^5	3.17×10^4	1.52×10^5	1.84×10^5
	310	336	5	3	0.02	2×10^4	—	2.64×10^4	1.97×10^5	2.24×10^5
10	198	144	10	3	0.0355	—	2.75×10^5	9.40×10^2	3.19×10^5	3.20×10^5
9	206	72	15	10	0.0897	—	4.22×10^5	8.65×10^3	4.18×10^5	4.27×10^5

**Fig. 8** Neural network predictions of fatigue life with increasing stress amplitude and comparison with the analytical models and experimental data.**Fig. 9** Neural network predictions of fatigue life with increasing frequency of loading and comparison with the experimental data.

loading varied from 1.25 to 20 cycles/day. Figure 9 presents the initiation and propagation life as a function of the loading frequency. Other parameters for this simulation are $\Delta\sigma = 180$ MPa, $R = 0.1$, $a_{ci} = 0.112$ mm, $a_f = 3$ mm, and $a_0 = 0.001$ mm. The duration of exposure D_{exp} was 144 h. The cross mark in Fig. 9 indicates the experimental result for the case with a similar specimen with a frequency of 198 MPa. The failure life increases from 8.50×10^4 to 4.2×10^5 cycles when the frequency is increased from 1.25 to 20 cycles/day. Because of a lack of information in the literature, the hold time and shape of the waveform was not considered in this study. However, for a realistic simulation, the hold time and waveform shape should be considered when discussing the frequency effect on fatigue life.

D. Discussion

The neural network model developed in this study is able to predict the final fatigue failure life of the panels with corrosion fatigue fairly well, as shown in Tables 2–4 and Figs. 6–9. The results were compared with those predicted by the analytical model developed by Wang et al.,¹² as well as with other analytical and experimental data

available in the literature. The results of simulations with varying parameters of pit size, stress amplitude, and frequency of loading are presented, and their effect on fatigue life was discussed.

V. Conclusions

The present study is aimed at investigating the pitting corrosion classification and distribution and predicting the corrosion-fatigue life of aircraft aluminum panels. A PNN was developed to classify the pit size distributions based on the available experimental data. The pit size range was classified into three groups and distributions were fit to those three pit size ranges. Overall, the gamma distribution function fitted very well to the experimental data for the three ranges of pit sizes. Also, a neural network model was developed for predicting the fatigue life of aircraft panels subjected to corrosion-fatigue loading. The developed neural network model was validated against the experimental data and other analytical methods available in the literature. Overall, the neural network predictions compared reasonably well with the experimental data. Few simulations were carried out to predict the fatigue life of panels subjected to different damage environments. The results were compared to those predicted by analytical models. The predictions of the present model were fairly accurate for most of the panels studied, given the inherent statistical variation of fatigue data. Overall, this study demonstrates the use of neural networks for estimating the fatigue life of aircraft structures.

From a practical point of view, the developed neural network methodology has the following advantages and limitations. Trained neural networks from various data sources can generalize the fatigue phenomena and can predict fatigue life very efficiently and easily. If one is not interested in the crack initiation life, the critical pit size that initiates a fatigue crack is not important in the model. However, it might help in knowing how much of a portion of fatigue life is taken for initiation as compared to propagation life, which is important for high-cycle fatigue. Also, the final crack size, as defined in the model, can be used as a detectable crack by nondestructive inspection techniques. The fatigue life predictions obtained from the present methodology can be used as an aid in evaluating the remaining life or to schedule the next inspection in the maintenance program. To make the present methodology into a useful and safe tool for fatigue predictions, much more work has to be done. Currently, we are extending the present methodology into redesigning the operative environment to have specific fatigue properties for an aging aircraft structure/component.

Acknowledgments

The authors thank the National Science Foundation (NSF) for funding this research through grant CMS-9812723. Chris Sowers is supported by the NSF-(Research Experience for Undergraduates) program with Ken Chong as the program director.

References

- Wallace, W., and Hoepfner, D. W., *AGARD Corrosion Handbook Volume I Aircraft Corrosion: Causes and Case Histories*, AG-278, AGARD, 1985.
- Wei, R. P., Liao, C. M., and Gao, M., "A Transmission Microscopy Study of 7075-T6 and 2024-T3 Aluminum Alloys," *Metallurgical and Materials Transactions A*, Vol. 29A, 1998, pp. 1153–1160.
- Pao, P. S., Feng, C. R. J., and Gill, S. J., "Corrosion-Fatigue Crack Initiation in 7000-series Al Alloys," *Second Joint NASA/FAA/DoD Conference on Aging Aircraft*, Pt. 2, 1999, pp. 831–840.

⁴Hoeppner, D. W., "Model for Prediction of Fatigue Lives Based Upon a Pitting Corrosion Fatigue Process," *Fatigue Mechanisms*, STP 675, American Society for Testing and Materials, Philadelphia, 1979, pp. 841–863.

⁵Wei, R. P., Li, C., Harlow, D. G., and Flournoy, T. H., "Probability Modeling of Corrosion Fatigue Crack Growth and Pitting Corrosion," *ICAF 97: Fatigue in New and Aging Aircraft*, edited by R. Cook and P. Poole, Vol. 1, 1998, pp. 197–214.

⁶Harlow, D. G., and Wei, R. P., "Probabilities of Occurrence and Detection of Damage in Airframe Materials," *Fatigue and Fracture of Engineering Materials and Structures*, Vol. 22, No. 6, 1999, pp. 427–436.

⁷Harlow, D. G., and Wei, R. P., "A Probability Model for the Growth of Corrosion Pits in Aluminum Alloys Induced by Constituent Particles," *Engineering Fracture Mechanics*, Vol. 59, No. 3, 1998, pp. 305–325.

⁸Harlow, D. G., and Wei, R. P., "Probability Approach for Prediction of Corrosion and Corrosion Fatigue Life," *AIAA Journal*, Vol. 32, No. 10, 1994,

pp. 2073–2079.

⁹Rokhlin, S. I., Kim, J. Y., Nagy, H., and Zoofan, B., "Effect of Pitting Corrosion on Fatigue Crack Initiation and Fatigue Life," *Engineering Fracture Mechanics*, Vol. 62, No. 4–5, 1999, pp. 425–444.

¹⁰Zamber, J. E., and Hillberry, B. M., "Probabilistic Approach to Predicting Fatigue Lives of Corroded 2024-T3," *AIAA Journal*, Vol. 37, No. 10, 1999, pp. 1311–1317.

¹¹Wang, Q. Y., Berard, Y. J., Rathery, S., and Bathias, C., "High Cycle Fatigue Crack Initiation and Propagation Behavior of High Strength Spring Steel Wires," *Fatigue and Fracture of Engineering Materials and Structures*, Vol. 22, No. 8, 1999, pp. 673–677.

¹²Wang, Q. Y., Pidaparti, R. M., and Palakal, M. J., "Comparative Study Corrosion Fatigue in Aircraft Materials," *AIAA Journal*, Vol. 39, No. 2, 2001, pp. 325–330.

¹³Demuth, H., and Beale, M., "Neural Network Toolbox: For Use with MATLAB, User's Guide," Ver. 3.0, Jan. 1998, pp. 1-2–1-20 and 6-12–6-15.